CONCEPTUAL MEASUREMENT OF INDIVIDUAL PITCHES DURING THE STENT PRODUCTION

Benedikt Haas and Eric Sax
Institute for Information Processing Technologies (ITIV)
Karlsruhe Institute of Technology (KIT)
Karlsruhe, Germany

ABSTRACT

Due to cardiovascular diseases being the main cause of death in Germany in 2020, about 298,557 stents, which can be used to treat these kinds of diseases, were implanted. Stents are medical devices and therefore, need to fulfill corresponding requirements. The requirements, like the geometric form, have to be checked. In practice, in the case of maypole braided stents, this will be performed manually. In order to be more cost-efficient, an automatic visual inspection system is desirable. The proposed concept, representing such a system, consists of six steps: 1) image preprocessing, 2) mandrel detection, 3) dynamic image cropping, 4) pitch measurement, 5) pitch localization, and 6) modeling. Additionally, it allows to measure individual segments of the stent, enabling a precise error localization. Furthermore, the algorithm is designed to be executed during production. Lastly, the industrial environment, as well as requirements, are incorporated, such that an existing product diversity is not restricted.

KEYWORDS

Stents, Machine Vision, Pitch Measurement, Image Processing

1. INTRODUCTION

In the year 2020, in Germany, reportedly 985,572 citizens died. The reason of death for 330,001, which equals 36.4%, of them, are diseases of the cardiovascular system. (Radtke, 2023) One possible treatment for these diseases is an implantation of a stent (Wintermantel et al, 2008). Therefore, in Germany, in 2020, 298,557 stents were implanted (Herzstiftung eV, 2021). According to the German fee-per-case system, the costs for a stent range from 54.80€ to 1,189.69€, depending on the specific stent (InEK GmbH, 2021). One possible reason for these high costs could be the absence of an automatic visual inspection system for (maypole) braided stents (Bermudez, 2017).

This paper proposes a concept for an automatic visual inspection system of single segments of a (maypole) braided stents during production. In specific, it aims to measure the geometric size of the single segments. Therefore, it contributes to the field of automatic quality control and/ or visual inspection systems in the context of an automated stent production.

2. STENTS AND STENT PRODUCTION

The stents relevant to this work are tubular or circular braids produced by a maypole braider (see Figure 1). Its two main components are the carriers and the mandrel. The carriers store the braiding wire, which is connected to the mandrel. When the braiding process starts, the carriers move in a sinewave path around the mandrel, in pairwise opposite directions. During this process, the mandrel moves upwards. Its movement speed is called take-off speed. In addition, a braiding ring can be used optionally. It'll help regulate the braiding process. In the resulting mesh structure, as shown in Figure 2, a single mesh is called a pitch. A pitch can be described using its length and width. The pitch length is the distance between the topmost and bottommost interlacing point of the wire of a pitch. Equivalently, the pitch width is the distance between the leftmost and rightmost interlacing points of the wire. (Koysev, 2014)

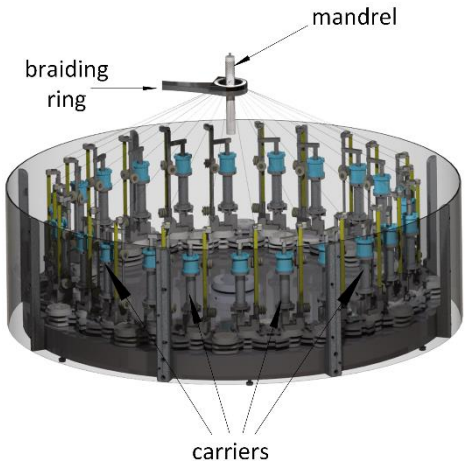

Figure 1. Schematic visualization of a Maypole braider. Marked are the mandrel, the carriers and the braiding ring

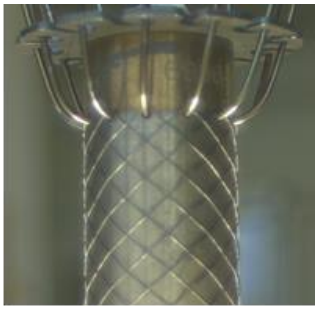

Figure 2. Image of a stent during production. Visible are the braided stent as well as the mandrel. (Haas et al, 2021)

3. RELATED WORK

The authors do not know of any approaches and/ or visual inspection systems for maypole braided stents.

Due to the fact, that stents are a specific type of braid, methods analyzing (general) braids could be transferred to the problem at hand. The most common method of analyzing these is to use a Fourier-based approach, like the discrete or fast Fourier transformation (Brigham/ Morrow, 1967) (see (Hunt, 2017), (Hunt/ Carey, 2019), (Vollbrecht et al, 2021), (Ershov, 2022) or (Jiyong et al, 2023)). Less common are:

- the Hough transformation (Duda/ Hart, 1972) being used in (Schmitt/ Mersmann/ Schoenberg, 2009) or (Monnot/ Levesque/ Lebel, 2017),
- a spectral analysis, like proposed from (Zhenkai/ Jialu, 2006), or
- an approach based on convolutional neural networks, like shown in (Şerban/ Barsanescu, 2020).

Additionally, (Hunt/ Carey, 2019) and (Vollbrecht et al, 2021) performed a measurement at the time of production, while (Şerban/ Barsanescu, 2020), (Vollbrecht et al, 2021) and (Jiyong et al, 2023) used the measurement result(s) in some sort of feedback loop to control the braiding system.

All mentioned methods have in common, that the environment was controlled or ideal. In addition, the measurement results weren't used in any kind of modeling. Therefore, a precise error localization wasn't possible. Furthermore, a single measurement was performed using multiple picks. This will smooth the measured values, which will introduce a (measurement) bias. Lastly, the content of the used images is different regarding the number of visible wires. This will influence the number of lines and edges in the image and therefore, the measurement method.

4. REQUIREMENTS

(Haas/ Erlinghagen/ Sax, 2022) already defined requirements regarding the measurement error as well as the execution time. Relevant to this paper are:

- that the maximal execution time of the measurement system has to be small enough, such that every pitch is seen at least once,
- that the image's middle falls onto the mandrel and
- that the mandrel is a cylinder and vertically aligned (with the camera's field of view).

Additionally, the measurement system should not restrict the production process. This does explicitly include production resources like the braiding wire and the mandrel.

5. CONCEPT

In order to solve this, the in Figure 3 shown algorithm is proposed. It consists of roughly six steps. These steps are 1) image preprocessing, 2) mandrel detection, 3) dynamic image cropping, 4) pitch measurement, 5) pitch localization, and 6) modeling.

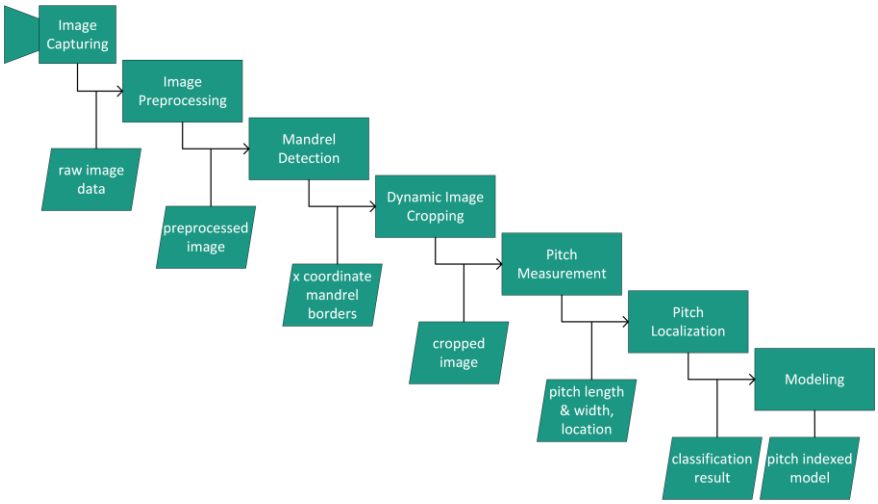

Figure 3. Visualization of the proposed concept including (measured and/ or generated) artifacts

5.1 Image Preprocessing

The image preprocessing receives the raw image data from the camera, which performs the image capturing. Therefore, the raw data has to be converted into a suitable format, like for example RGB. This is done using a demosaicing algorithm. The specific implementation of this algorithm is camera-dependent. While it is camera specific, there are different types of demosaicing algorithms. These range from fast and artifact bias ones like a bilinear interpolation, to slower approaches like the variable number of gradients (VNG), which contains fewer artifacts. (Malvar/ He/ Cutler, 2004) Therefore, the used method is system specific and is dependent on requirements like real-time conditions as well as the allowed measurement error.

5.2 Mandrel Detection

In order to crop the image, it is necessary to know, where the object being measured is. Due to the positioning of the camera relative to the mandrel being noised, this has to be measured. The mandrel being a cylinder, which is assumed to be vertical, it can be described using the left and right border. Each border being a line, can be defined using two two-dimensional points. Because of the verticality of the border, the y coordinate can

be disregarded. Additionally, if the mandrel is not skewed, then the lines are parallel to the y-axis. In this case, the x coordinates of both points are identical and only one of them has to be stored. In practice, if the mandrel is skewed or the measurement is noised, then a faulty border is to be expected. Due to the borders being used in the image cropping, faulty borders will lead to faulty image cropping. The result of faulty image cropping can be 1) a too-small cropped image, 2) a too-big cropped image, 3) a false cropping position, or 4) the cropped image contains background. Especially the last point (4) can lead to (huge) measurement errors due to the background influencing the pitch measurement. 1) and 2) can be dealt with by defining minimal and/ or maximal sizes based on prior knowledge about the pitches and the mandrel. Because the borders only influence the horizontal position, a consistency check using the image's middle can be performed and prevent a cropping position (3), which does not include the preprocessed image's middle. If it (the image's middle) is included, it is highly likely, that at least one measurable pitch is shown in the cropped image. Due to these reasons, only one x coordinate will be used the describe a mandrel border.

In a practical implementation, the measurement can be performed using a variety of image processing algorithms. In general, these algorithms consist of three steps, namely (Stiller/ Bachmann/ Duchow, 2009): 1) image preprocessing, 2) feature extraction, and 3) Information extraction. The mapping of specific methods or algorithms to one of the three steps cannot be done in general. However, there are some algorithms or methods which are preferably used in one of those steps. E.g. image filtering like blurring (Beyerer/ León/ Frese, 2016) or using the Sobel operator (Kanopoulos/ Vasanthavada/ Baker, 1988), is usually done in the scope of the image preprocessing. Additionally, methods like the Hough transformation or the Canny operator (Canny, 1986) are used to extract lines or edges. Because lines or edges represent the borders of one or multiple objects, they are categorized as features. Therefore, such algorithms are usually part of the feature extraction. Lastly, methods that extract the desired information are part of the information extraction. This includes e.g. computing the intersection point(s) of lines or counting pixels in order to measure a distance.

Additionally, it is known, that the mandrel is placed in the image's middle (see chapter 4). Using this information, the search space for each border can be restricted to the corresponding half of the image. In addition, the measured borders can be checked for consistency using said information, as well as being in the range of the image dimensions. Moreover, an area, where the borders should be found, can be defined using previous knowledge and/ or the diameter of the mandrel, offering another possibility for a consistency check.

5.3 Dynamic Image Cropping

Using the mandrels borders, the image can be cropped, like presented in (Haas/ Erlinghagen/ Sax, 2022). This approach focuses on a sub-image creation, which contains the same amount of information and got the same dimensions. Due to the reason, that the images show multiple pitches as well as a mandrel, a regulation of the amount of information results in regulating the number of visible pitches. Obviously, the image has to include at least one pitch. Otherwise, there wouldn't be any measurable pitch present. In order to always contain a complete pitch, the size of the cropped image is set to three times the expected size of a pitch. It is necessary because the to-be-measured pitch includes the image's middle but does not have to be centered around it. This results in a sub-image with a size 3×3 expected pitch size, rather than containing 3×3 complete pitches. After the cropping, the sub-image is resized to a fixed size like 512×512. This will result in sub-images, that contain about the same amount of information as well as have the same image dimensions.

Alternatively, the image could be cropped using a fixed-sized rectangle. This would lead to sub-images, which contain a different number of pitches. The specific number is dependent on the pitches' size as well as the rectangles' size. Because the image has to contain at least one measurable pitch, the size will correspond to the size of the biggest measurable pitch. At the same time, in the case of smaller pitch sizes, this will lead to the display of a great number of pitches. If methods based on e.g. Convolution Neural Networks (CNNs) should be used, this can lead to measurement errors due to the variety. Additionally, the generated sub-images of different measurements are not comparable, which could lead to a lack of trust from a potential user as well as an additional problem dimension. Following this, the amount of information (aka pitches), has to be regulated, resulting in sub-images of different sizes. Rescaling these sub-images will lead to noise due to either the compression ("downscaling") or the generation ("upscaling") of the image. Nonetheless, scaling to a fixed size will produce comparable sub-images, which is human-friendly. Additionally, methods, which are based on e.g. CNNs, expect inputs to have the same size and therefore require a rescaling. Lastly, the multiplication factor is used to ensure, that at least one pitch is shown completely and therefore, measurable. It is necessary because

1) the size of the interlacing points is not part of the pitch length and/ or width and 2) the pitch does not have to be centered in the sub-image. 2) can be achieved using a multiplication factor greater than two, as shown in (Haas/ Erlinghagen/ Sax, 2022). At the same time, the factor should be as small as possible. The greater the factor, the greater the sub-images will be and therefore increase the likelihood of a downscaling. Following this, using a factor of three is a reasonable compromise. Additionally, using three covers 1). Moreover, if the expected size of the pitch is unknown, the measurement system cannot be used. This can be approached using the previously measured pitch size instead. Therefore, only an estimation for the first pitch being measured is needed. Lastly, the target dimension of the scale influences the measurement performance. On the one hand, if the target dimension is too small, then the information loss caused by the downscaling will result in a bad measurement performance. On the other hand, if it is too big, artifacts, due to the upscaling, will bias the measurement. Additionally, an increase in image size will lead to higher resource costs and a higher execution time. In the end, the size of 512×512 was chosen due to its popularity in Frameworks like PyTorch (Paszke et al, 2019) or Tensorflow (Abadi et al, 2015).

5.4 Pitch Measurement

Based on these sub-images, a pitch measurement can be implemented. Due to the sub-image being designed to contain one measurable pitch in its middle, the goal of the pitch measurement is to measure the pitch in the sub-images middle. In specific, the target is to compute the pitch length and width, as well as some kind of spatial information. Due to the image being two-dimensional, the location can be described using one two-dimensional coordinate. The process of extracting the pitch length and width as well as its location is equivalent to the one described in chapter 5.2.

5.5 Pitch Localization

The next step, namely the pitch localization, computes the index of the measured pitch dependent on the previously measured ones. In order to be resource efficient as well as have a low execution time, this computation won't be image-based. It'll use the measured location of the current, as well as the previously measured pitch. This will reduce the amount of computation time needed from analyzing at least one image to analyzing two (two-dimensional) locations. Specifically, the location of the previously measured pitch will be propagated to the current point in time using the mandrel's take-off speed as well as the time difference between both measurements. Then, the difference between the current and the propagated location can be interpreted as a difference vector. Incorporating the requirements (see chapter 4), the number of possible indices and therefore, the values (or space) of the difference vectors, are restricted. In detail, the difference vector can be mapped onto nine different indices, as shown in Figure 4. Due to this restriction, the computation of the measured pitches index can be interpreted as a classification task, using the described difference vector. In this classification scheme, class 5 represents the same pitch, while class 9 states, that the measured pitches row index equals the previous one plus two. Examples of methods being able to perform such a classification task are a multi-class SVM (Vapnik, 1963), a decision tree, a random forest (Ho, 1995), or a neural network.

The described approach is iterative; therefore, an alternative would compute the index directly. In order to do so, the complete stent would have to be visible. Otherwise, the computation would be state dependent and iterative. In practice, the complete stent does not have to be visible/ in the camera's field of view. Therefore, this approach is, in practice, not feasible. Even if the complete stent would be visible, it would require analyzing the complete image, which is cost and time inefficient. Also, cost and time inefficient would be, to compute the index iteratively using two cropped images, especially compared to the analysis of two different locations. Additionally, using a classification schema instead of computing the index directly, has the advantage, that a (classification) confidence can be provided. In the case of an error, it (the confidence values) can be used to locate said error. Moreover, if the column (index) is neglected, the confidence values can be summed up representing one row.

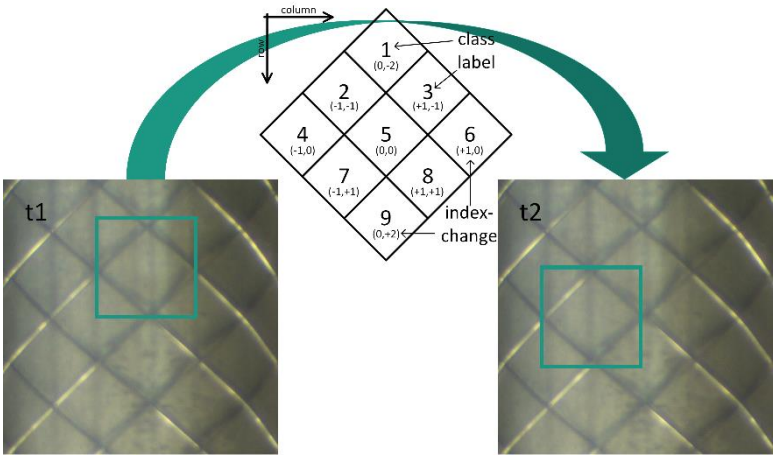

Figure 4. Visualization of the classification scheme used in the pitch localization embedded into an example. In this example, the pitch change from t1 to t2 results, according to the schema, in class 7

5.6 Modeling

The last step is to transform the output of the pitch measurement as well as localization into a consistent representation. Due to the localization being pitch indexed, the resulting model will be the same. Additionally, there will probably be multiple measurements of the same pitch. Therefore, these measurements have to be combined such that one pitch is represented by a single value. This can be done using the median of the measured length and width of the pitch. Compared to the mean, the median is more robust regarding noise and outliers, and therefore the preferred solution. The location information is, in contrast to the pitch length and width, time-sensitive. Additionally, it can be regarded as an interim result. Therefore, it can be saved for traceability reasons or otherwise, be discarded. Lastly, the measurement values can optionally be converted from pixel to an SI unit. The mapping to e.g. millimeters can be retrieved using the mandrel's diameter as well as the distance between the (measured) borders of the mandrel.

6. PROOF OF CONCEPT

The presented concept was implemented in C++ and tested, using data produced by a commercial maypole braider. This was done in cooperation with an industrial partner, in the scope of the project Stents4Tomorrow. As a result, the mandrel detection using a Hough Transformation and the pitch measurement, being realized with a YoloV3 object detector, had a mean measurement error of 2,64 mm (MAPE: 13,2%) and 0,58 mm (pitch length, MAPE: 7,7%) with a mean execution time of 127,55 ms and 66,32 ms. The localization, which was based on the k-nearest neighbors algorithm, achieved an accuracy of 99,99% while needing 0,24 ms on average.

7. CONCLUSION

Analyzing the described measurement process, there are some parts, which could prevent a (successful) practical implementation. The first one is the neglection of a skewed mandrel. This problem can be solved using some kind of camera-mandrel alignment. Such an alignment has to influence the position of the camera because the mandrel's location is fixed. In addition, a falsely set take-off speed will influence the localization leading to, in the worst case, a localization error. This does include the (mandrels) acceleration process, which, if not modeled, will lead to a wrong assumption about the take-off speed value. But, due to the acceleration process being machine-specific, modeling it would not be satisfying. Therefore, the used classification method has to be robust regarding this kind of noise. Alternatively, the take-off speed could be measured. This requires

the analysis of two images, which is resource and execution-time inefficient. In addition, using a method, which computes a decision confidence, could offer some transparency in the case of a measurement error. Moreover, the concept does not incorporate measurement errors caused by production diversity, changes in the environment as well as software-based ones. Having said this, the color information can (probably) be disregarded using appropriate color space transformations. While changes in the environment will influence at least the image quality, methods like a histogram equalization can try to compensate for those. Finally, the concept assumes, that the image contains a mandrel and pitches, which is, especially at the beginning of a braiding process, not always true. Therefore, a sub-process, handling the absence of a mandrel and/ or pitches, should be included.

8. SUMMARY & OUTLOOK

In this paper, an algorithm to measure single pitches of a stent, during its production, is proposed. This algorithm contains roughly six steps, namely:

1. Image preprocessing: The method unspecific preparation of the image,
2. Mandrel detection: Image-based measurement of the location of the mandrel's borders,
3. Dynamic image cropping: Cropping of the image to contain the same amount of information as well as having the same size,
4. Pitch measurement: The measurement of the pitch length and width as well as its location,
5. Pitch localization: The computation of the index of the measured pitch and
6. Modeling: The conversion into a consistent representation including the handling of multiple measurements of the same pitch.

Using this procedure, the geometric size of single pitches of a stent can be measured. Following this, the deviation regarding the target geometry (pitche's length and width) can be computed. Additionally, due to the comparison with the target geometry, it will implicitly detect missing pitches.

Future work could thematize the problems mentioned in chapter 7. Additionally, the integration of non-cylindrical mandrels into the described process could be analyzed. Alternatively, the process could be implemented and different methods evaluated in order to satisfy the requirements. In this case, the production diversity, like the pitch length and width, the mandrels diameter as well as the wire's color and diameter, should be included.

ACKNOWLEDGEMENT

Parts of this work have been developed in the project Stents4Tomorrow. Stents4Tomorrow (reference number: 02P18C022) is partly funded by the German ministry of education and research (BMBF) within the research program ProMed. Additionally, the authors want to thank M. Braeuner (Admedes GmbH) and K. Lehmann (Admedes GmbH) for their continuous support and advice.

REFERENCES

Abadi, M., et al., 2016, Tensorflow: Large-scale machine learning on heterogeneous distributed systems. arXiv preprint arXiv:1603.04467.

Bermudez, C. et al., 2017, Automated stent defect detection and classification with a high numerical aperture optical system. In Automated Visual Inspection and Machine Vision II. SPIE. S. 92-102.

Beyerer, J.; León, F.P.; Frese, C., 2016, Automatische Sichtprüfung: Grundlagen, Methoden und Praxis der Bildgewinnung und Bildauswertung. Springer-Verlag.

Brigham, E. O., Morrow, R. E, 1967, The fast Fourier transform. IEEE spectrum, 4. Jg., Nr. 12, S. 63-70.

Canny, J., 1986, A computational approach to edge detection. IEEE Transactions on pattern analysis and machine intelligence, Nr. 6, pp. 679-698.

Duda, R. O., Hart, P.E., 1972, Use of the Hough transformation to detect lines and curves in pictures. In Communications of the ACM, 15. Jg., Nr. 1, S. 11-15.

Ershov, S. V., et al., 2022, Method for Measuring the Braid Angle and its Deviation from the Specified Value in Braided Preforms Using Image Analysis. Fibre Chemistry, 53. Jg., Nr. 5, S. 346-354.

Haas, B., et al., 2021, Evaluation of different methods to measure a stent's pitch length in an industrial environment. In: 2021 International Conference on Electrical, Computer, Communications and Mechatronics Engineering (ICECCME). IEEE, S. 1-6.

Haas, B., Erlinghagen, L., Sax, E., 2022, Pitch length measurement of stents using dynamically cropped images. In: 2022 International Conference on Electrical, Computer, Communications and Mechatronics Engineering (ICECCME). IEEE, pp. 1-6.

Herzstiftung eV, D. 2021. Deutscher Herzbericht 2020. Frankfurt am Main: Deutsche Herzstiftung eV, 2021-06.

Ho, T. K., 1995. Random decision forests. In: Proceedings of 3rd international conference on document analysis and recognition. IEEE, pp. 278-282.

Hunt, A. J. A, 2017, Machine Vision System for the Real-Time Fiber Orientation Measurement of Tubular Braided Preforms.

Hunt, A.J.; Carey, J.P., 2019, A machine vision system for the braid angle measurement of tubular braided structures. In Textile Research Journal, 89. Jg., Nr. 14, S. 2919-2937.

InEK GmbH – Institut für das Entgeltsystem im Krankenhaus, 2021, aG-DRG-Fallpauschalen-Katalog 2022, [online] https://www.g-drg.de/content/download/10834/file/Fallpauschalenkatalog_2022_20211123.pdf [visted 2023-03-13].

Jiyong, F. et al., 2023, Traction control of space tubular shaped mandrel and detection of preform braiding angle. In Textile Research Journal, 93. Jg., Nr. 1-2, S. 392-408.

Kanopoulos, N., Vasanthavada, N., Baker, R.L, 1988, Design of an image edge detection filter using the Sobel operator. IEEE Journal of solid-state circuits, 23. Jg., Nr. 2, pp. 358-367.

Koysev, Y., 2014, Braiding technology for textiles: Principles, design and processes. Elsevier.

Monnot, P.; Levesque, J.; Lebel, L.L., 2017, Automated braiding of a complex aircraft fuselage frame using a non-circular braiding model. Composites Part A: Applied Science and Manufacturing, 102. Jg., S. 48-63.

Paszke, A. et al, 2019, PyTorch: An Imperative Style, High-Performance Deep Learning Library, Advances in Neural Information Processing Systems 32, pp. 8024-8035.

Radtke, R. 2023. Anzahl der Todesfälle nach den häufigsten Todesursachen in Deutschland in den Jahren 2019 bis 2021. Statista.

Şerban, A.; Barsanescu, P.-D., 2020, Automatic detection of fibers orientation on composite laminates using convolutional neural networks. In: IOP Conference Series: Materials Science and Engineering. IOP Publishing, pp. 012107.

Stiller, C.; Bachmann, A.; Duchow, C., 2009, Maschinelles Sehen. Handbuch Fahrerassistenzsysteme: Grundlagen, Komponenten und Systeme für aktive Sicherheit und Komfort, pp. 198-222.

Malvar, H.S.; He, L.-w.; Cutler, R., 2004, High-quality linear interpolation for demosaicing of Bayer-patterned color images. In: 2004 IEEE International Conference on Acoustics, Speech, and Signal Processing. IEEE, pp. iii-485.

Monnot, P.; Levesque, J.; Lebel, L.L., 2017, Automated braiding of a complex aircraft fuselage frame using a non-circular braiding model. Composites Part A: Applied Science and Manufacturing, 102. Jg., S. 48-63.

Vapnik, V., 1963, Pattern recognition using generalized portrait method. Automation and remote control, 24. Jg., pp. 774-780.

Vollbrecht, B. et al., 2021, Developing a camera-based measuring system to feedback control the fibre orientation for the braiding process of CFRP. In Advances in Industrial and Manufacturing Engineering, 3. Jg., S. 100059.

Wintermantel, E. et al, 2008, Stenting und technische Stentumgebung. In Medizintechnik Life Science Engineering: Interdisziplinarität· Biokompatibilität· Technologien·Implantate·Diagnostik Werkstoffe Business, pp. 1009-1041.

Zhenkai, W., Jialu, L., 2006, Braided angle measurement technique for three-dimensional braided composite material preform using mathematical morphology and image texture. AUTEX Research Journal, 6. Jg., Nr. 1, pp. 30-39.